



**University of  
Zurich**<sup>UZH</sup>

**Zurich Open Repository and  
Archive**

University of Zurich  
University Library  
Strickhofstrasse 39  
CH-8057 Zurich  
[www.zora.uzh.ch](http://www.zora.uzh.ch)

---

Year: 2020

---

## **Droplet assisted growth and shaping of alumina and mixed alumina-silicone 1-dimensional nanostructures**

Saddiqi, Naeem-ul-Hasan ; Seeger, Stefan

**Abstract:** Since the discovery of silicone nanofilaments a decade ago, room temperature droplet assisted growth and shaping using silanes has been used to synthesize various silicone-based nanostructures. In the present work, we report an extension of this synthesis technique to synthesize nanostructures of new materials. We have successfully synthesized one-dimensional assemblies of beads or necklaces based on alumina (Al) and mixed alumina-silicone (Al Si) nanostructures exhibiting a similar structure as silicone nanofilaments. The characterization of the synthesized nanostructures was performed using different tools, including scanning and transmission electron microscopy, energy dispersive x-ray spectroscopy, and infrared and NMR spectroscopy. Selected area electron diffraction revealed that the nanostructures are amorphous in nature, and the growth behavior and thermal stability of nanostructures are also discussed

DOI: <https://doi.org/10.1016/j.jcis.2019.09.122>

Posted at the Zurich Open Repository and Archive, University of Zurich

ZORA URL: <https://doi.org/10.5167/uzh-183311>

Journal Article

Accepted Version



The following work is licensed under a Creative Commons: Attribution-NonCommercial-NoDerivatives 4.0 International (CC BY-NC-ND 4.0) License.

Originally published at:

Saddiqi, Naeem-ul-Hasan; Seeger, Stefan (2020). Droplet assisted growth and shaping of alumina and mixed alumina-silicone 1-dimensional nanostructures. *Journal of Colloid and Interface Science*, 560:77-84.

DOI: <https://doi.org/10.1016/j.jcis.2019.09.122>

# Droplet Assisted Growth and Shaping of Al and Mixed Al-Si 1D Nanostructures

Naeem-ul-Hasan Saddiqi, Stefan Seeger\*  
Department of Chemistry, University of Zurich, Winterthurerstr. 190,  
8057 Zurich, Switzerland

\*corresponding author: [sseeger@chem.uzh.ch](mailto:sseeger@chem.uzh.ch)  
Phone: +41 44 635 44 51

## Abstract

Since the discovery of silicone nanofilaments a decade ago room temperature droplet assisted growth and shaping using silanes has been used to synthesize various silicone based nanostructures. In the present work we report an extension of this synthesis technique to synthesize nanostructures of new material. We have successfully synthesized one dimensional assemblies of beads or necklaces based on Al and mixed Al-Si nanostructures exhibiting a similar structure as silicone nanofilaments. The characterization of synthesized nanostructures has been performed using different tools such as scanning and transmission electron microscopy, energy dispersive x-ray spectroscopy, infrared and NMR spectroscopy. Selected area electron diffraction has revealed nanostructures are amorphous in nature. The growth behavior and thermal stability of nanostructures have also been discussed in this report.

**Keywords:** Droplet assisted growth and shaping; silicone nanofilaments; nanostructures; chemical vapor deposition; room temperature synthesis

## Introduction

The synthesis of nanostructures generates a large number of exciting opportunities due to their small size and high surface area. The ability to store gas in nano-sized pores of silica<sup>[1]</sup> or in the field of microelectronics<sup>[2]</sup> where performance is inversely related to the size, are successful examples of application of nanomaterials in real life. With the better understanding of synthesis

and material properties nanostructures possessing different shapes and dimensions have been fabricated. One dimensional (1D) nanostructures in the form of wires, rods, fibers or tubes are an example of nanomaterials which have attracted numerous attention because of their unique properties and applications in various fields<sup>[3]</sup>. These 1D nanostructures have been synthesized using top down approaches such as focused ion beam (FIB) writing<sup>[4]</sup>, x-ray or UV lithography and proximal probe patterning<sup>[5]</sup>, and bottom up approach for example liquid phase synthesis<sup>[6]</sup>, sol-gel<sup>[7]</sup>, electrospinning<sup>[8]</sup> and chemical vapor deposition (CVD)<sup>[9]</sup>. Further development of these methods for production on a large scale for range of materials at low cost still requires great innovation. CVD is one type of technique which has been used for the synthesis of different 1D nanomaterials such as carbon nanotubes (CNTs)<sup>[9]</sup>, silicon nanowires (SiNWs)<sup>[10]</sup> and other 1D nanostructures<sup>[11][12]</sup>. However most of these techniques require application of high operating temperature increasing the cost and making the process less energy benign. The possibility of synthesis of nanostructures at room temperature at ambient pressure is an energy efficient alternative process.

Ambient conditions can be applied to synthesize 1D nanostructures of silicone<sup>[13]</sup>. The synthesized 1D silicone nanostructures which are called silicone nanofilaments (SNFs) have a diameter in the order of a few nanometers and their length varies from nanometer to micrometer scale<sup>[14]</sup>. Further, a high variability in structures' shape could be obtained applying this method called "Droplet assisted growth and shaping" (DAGS) by simply adjusting the gas phase composition<sup>[15]</sup>. The advantage of this room temperature method lies in the fact such as energy efficiency, low cost, facile synthesis method, and ease in scalability and no liquid waste production<sup>[16]</sup>. Moreover, this synthesis technique can be used to grow nanostructures on various substrates<sup>[13][17][18]</sup>. SNFs have been found to be useful for a variety of applications which include superhydrophobic coatings<sup>[13][16]</sup>, super oleophobic coatings<sup>[19]</sup>, oil water separation<sup>[20]</sup>, catalysis<sup>[21]</sup>, biomineralization<sup>[22]</sup>, water disinfection<sup>[23]</sup>, and support for specific

protein adsorption<sup>[24]</sup>. The method is based on formation of the nano-droplets of water at the surface of substrate which determine the course of material growth..<sup>[25]</sup> The DAGS mechanism has been explored to synthesize silicone based micro and nanostructures in the form of stars, rods, spirals and helices by manipulating the surface chemistry of substrate<sup>[25][15]</sup>.

The DAGS chemistry is not only limited to silicone based materials but has recently been successfully applied to synthesize 1D nanostructures of germanium oxide<sup>[26]</sup>. The extension of the DAGS method to other material systems such as aluminum (Al) and mixed aluminum-silicone (Al-Si) is reported in this study. Al and mixed Al-Si based 1D nanostructures have been usually synthesized using various methods, e.g. hydrothermal method<sup>[27][28]</sup> or chemical vapor deposition<sup>[29]</sup> are a few examples; all of them involve application of high synthesis temperature and complex synthesis procedure. In this publication we describe for the first time the synthesis of aluminum and mixed aluminum-silicone based nanostructures using the DAGS synthesis principle. This is remarkable not only because it opens the door for simple straightforward synthesis of alumina-containing nanostructures. It also shows after successful synthesis of silicone- and germanium oxide-containing structures that the DAGS synthesis process is much more broadly applicable than just for one specific chemical substance class.

## **Materials**

Silicon wafers (100) (10 mm x 10 mm) and Germanium wafers (100) (10 mm x 10 mm) were obtained from Crystec GmbH (Berlin, Germany). Both wafer types were un-doped and single side polished. Microscopic glass slides (26 mm x 76 mm x 0.15 mm) were purchased from Menzel (Braunschweig, Germany). Acetone (technical grade), Trimethyl Aluminum (TMA) 2M solution in toluene, Trichloromethylsilane (TCMS) (purity 99%) and Toluene anhydrous (99.8%) were purchased from Sigma Aldrich (Buchs, Switzerland). De-ionized Milli-Q water (resistivity 18.2 MΩ·cm at 25 °C) was used for cleaning of wafers. All chemicals were used as received without any further purification.

### **Synthesis of Aluminum nanofilaments (AlNFs) using DAGS method**

To remove organic impurities from the surface, wafers were immersed in acetone for 30 minutes followed by washing with copious amount of acetone and Milli-Q water. Activation of the surface was performed in oxygen plasma chamber Femto from Diener Electronics (Nagold, Germany) at 100W power followed by washing with Milli-Q water to create (-OH) groups at the surface. The substrates were dried in the stream of N<sub>2</sub> gas. For the synthesis of AlNFs the already documented procedure was repeated which was applied for CVD of silicone nanofilaments (SNFs)<sup>13</sup>. In short, activated wafers were placed in glass desiccator and the relative humidity inside the chamber was adjusted at 35 %  $\pm$  1 % using the mixture of dry and humidified N<sub>2</sub>. The flow of the gas and relative humidity was controlled by EE23 (E + E Elektronik). Equilibration was carried out for 1 hour. The precursor (TMA 0.4 mmole) was taken with a pipette from glove box in an air tight glass vial and injected with a syringe inside the desiccator from the top septum to start the reaction. TMA is very reactive reagent and was handled in glove box with O<sub>2</sub> and H<sub>2</sub>O content below 1ppm. Reaction was carried out for the duration of 4 hours.

### **Synthesis of Aluminum-Silicone nanofilaments (Al-SiNFs) using DAGS method**

For the synthesis of Al-SiNFs, the wafers were cleaned and activated in the same manner as done for AlNFs synthesis. Relative humidity inside the glass chamber was maintained at 35 %  $\pm$  1 % for 1 hour. TMA (0.4 mmole) and TCMS (0.8 mmole) were taken with a pipette and mixed inside the glove box and transferred in an air tight glass vial. Precursors were injected from the septum inside the glass desiccator to start the reaction.

### **Study of Thermal Stability**

Annealing of samples was performed in air using Carbolite muffle furnace. Wafers were heated at 300°C, 400°C, 500°C and 600°C in air at the rate of 10°C/minute for duration of 4 hours followed by cooling in the furnace.

## **Characterization**

### **Scanning Electron Microscopy and Energy Dispersive X-ray Spectroscopy (EDX)**

Scanning electron microscopy (SEM) was done at the Center for Microscopy and Image Analysis (ZMB) of the University of Zurich on SUPRA 50VP electron microscope (Zeiss, Germany). All samples were coated with 10 nm thick platinum layer under high vacuum using Sputter Coater Safematic CCU-010 (Switzerland). Accelerating voltage of 4-6 keV was used to acquire images using secondary electron and in-lens detector. For energy dispersive x-ray spectroscopy (EDX), accelerating voltage of 6-10 keV was used with a sapphire Si (Li) detecting unit (EDAX Inc.). On average three measurements were taken for one sample under analysis.

### **Transmission Electron Microscopy and EDX Mapping**

Transmission electron microscopic images (TEM) were acquired using FEI Tecnai G2 Spirit with accelerating voltage of 120 KeV at ZMB University of Zurich. For EDX, X-Max system (Oxford) integrated with FEI Tecnai G2 spirit was utilized. For one map sample was scanned for 5-10 minutes and to get reliable data three to five maps per sample were collected. The samples were prepared by sonicating coated Si wafers for 3 minutes in 0.5 ml of anhydrous toluene. The ultrasound waves removed the nanostructures from the wafer and toluene solution was drop cast on TEM Cu grid for imaging and EDX analysis using TEM. Toluene used for sample preparation did not contain any impurities. To check the purity of toluene, it was drop cast on Cu grid and observed under TEM.

### **FTIR**

Fourier transform infra-red spectroscopy (FTIR) spectra were obtained from Bruker Vertex 70 using a Pike ATR accessory. Five spectra were acquired for each sample with 256 scans on every spectrum. The scanning resolution was maintained at 2 cm/sec.

## NMR

Solid state  $^{29}\text{Si}$  NMR spectra were recorded using Bruker MSL 500 spectrometer. Magnetic angle spinning was carried out at 25 kHz. All NMR spectra were calibrated to tetramethylsilane (TMS).

## Results and Discussion

### Synthesis of AlNFs

The synthesis of AlNFs has been executed on Si wafers, because of its ideal flat topography and easy availability. The coated Si wafers were analyzed by SEM to observe for any probable growth. The data obtained showed the presence of one dimensional (1D) nanostructures covering the whole wafer surface (Figure 1). The higher magnification revealed the 1D nanostructures are made of spherical-like shapes arranged in a necklace structure (Figure 1). EDX analysis of the as grown structures showed that they are essentially composed of Al and O, while Si and C signals are originated from the silicon wafer and carbon tape which was used to mount the wafer for SEM analysis.

TEM also shows 1D nanostructures and selected area electron diffraction (SAED) experiments reveal their amorphous nature (the inset Figure 2). Furthermore, EDX mapping of the synthesized nanostructures was also performed to see the distribution of elements inside the structures. Elemental mapping indicates the presence of Al and O inside the synthesized particles (Figure 2). Most likely the nanostructures are free of carbon as no contrast was observed in EDX mapping. Overall EDX spectra of the map is shown in **supporting info Figure 1** which reveals peaks of Al, O, C and Cu. The peaks of C and Cu are supposed to be from the TEM grid itself.

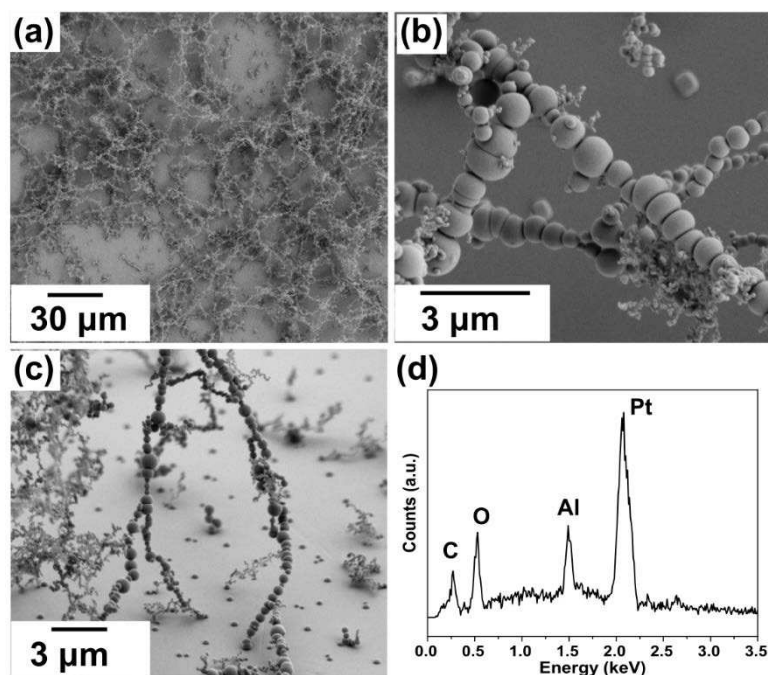


Figure 1: (a-c) As grown AlNFs observed under SEM, (d) EDX spectra of AlNFs

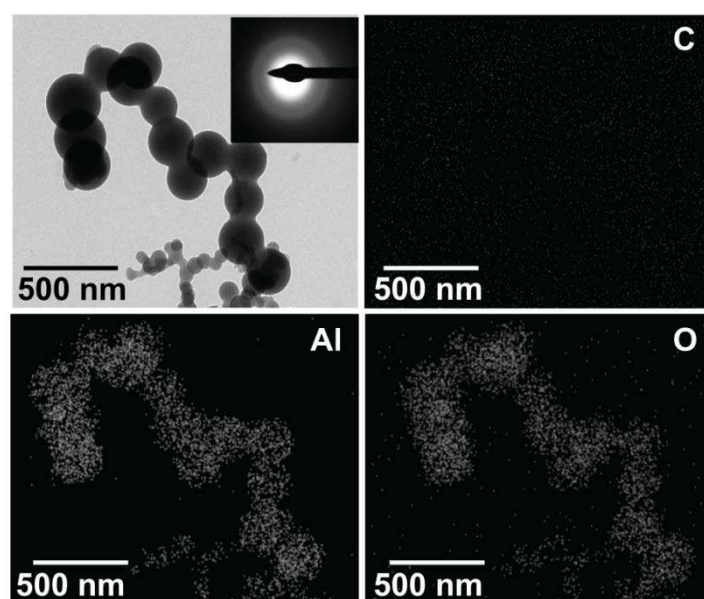


Figure 2: TEM image of AlNFs (inset SAED) and elemental mapping of AlNFs respectively.

Usually the synthesis of AlNFs was carried out at relative humidity level of  $35\% \pm 1\%$ , however to observe the influence of humidity on the growth of AlNFs synthesis at different humidity levels was also carried out, since this is a key parameter for SNF growth<sup>[15]</sup>. The humidity was varied from 2% to 70%, and the grown structures were observed using SEM. At low humidity levels especially 2% only sparse growth of AlNFs was observed (supporting info Figure 2).



With the increase of humidity the growth of AlNFs on the surface of substrate increases but at higher humidity levels of 50% and 70% random growth in the form of aggregated structures was also observed along with 1D AlNFs (supporting info Figure 2).

The TMA precursor is very reactive and reacts violently with water. When this precursor is used for the synthesis of nanostructures the humidity levels have to be adjusted carefully. In DAGS chemistry, the relative humidity inside the coating chamber plays an important role. When the substrate is placed in humid environment, it forms islands of water droplets at the surface of substrate. The islands of water are formed due to the inhomogeneity in the surface topography and chemical composition<sup>[30]</sup>. These nano water droplets act as confined reaction volumes. The precursor which is injected in the coating chamber vaporizes and reacts with the water droplet and with water in the gas phase. At low humidity levels the probability of forming water droplets at the surface of the substrate is low, i.e. limited growth of AlNFs is observed at low humidity level. With the increase of relative humidity the size and abundance of water droplets at the surface of the substrate increases leading to higher densities of AlNFs. However at high humidity levels of 50% (0.78 mmoles of H<sub>2</sub>O) and 70% (1.01 mmoles of H<sub>2</sub>O) the formation of larger water droplets and thin water layers lead to abrupt and uncontrolled reaction forming random and aggregated nanostructures at the surface.

We have also investigated the influence of reaction time on the growth of AlNFs. For this purpose reaction was stopped after 15 and 30 minutes of TMA injection. At short reaction time small particulate nanostructures were obtained. The coverage of the substrate was also low due to short reaction duration. With the increase in the duration of reaction nanostructures grow making 1D necklace or bead type structures (Figure 3).

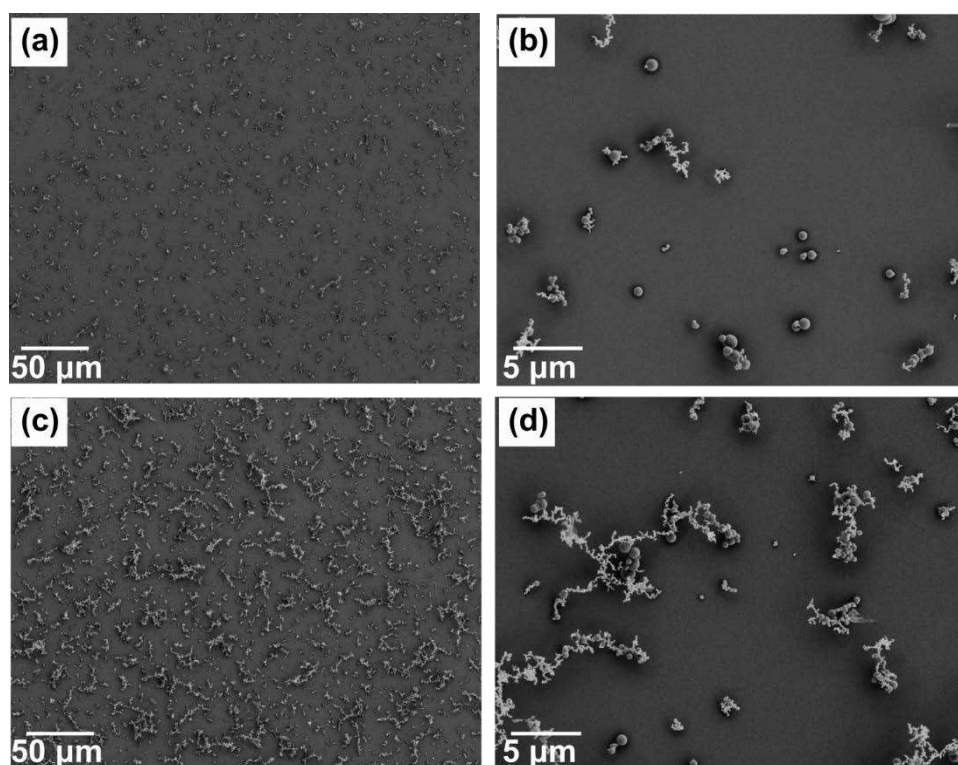


Figure 3: Growth of AlNFs after (a-b) 15 and (c-d) 30 minutes of reaction time

To check the thermal stability of as synthesized AlNFs on Si wafers, annealing of the substrates was performed in air. The surface of annealed wafers was observed using SEM. It was observed that AlNFs start to aggregate if the annealing temperature is increased from 300°C to 600°C (Supporting info Figure 3). With the increase of the annealing temperature sintering of the particles was also observed. The particles were amorphous in nature after annealing as shown in insets of supporting info Figure 4. EDX mapping shows no change in the composition of the particles after annealing (Supporting info Figure 4). Presence of Al and O was detected in all particles. Instead of using trimethylaluminum (TMA), triethylaluminum (TEA) was also employed to check the growth of 1D nanostructure. But due to its low vapor pressure (1mmHg at 62.2°C) it did not lead to successful growth of nanostructures (Supporting info Figure 5).

### Synthesis of Al-SiNFs

Trichloromethylsilane (TCMS) when used alone for chemical vapor deposition (CVD) leads to formation of 1D silicone nanofilaments (SNFs), while TMA leads to formation of AlNFs. To

observe the growth behavior when both of the precursors are used together, synthesis by mixing TCMS and TMA was carried out. For this purpose 0.4 mmoles of TMA were mixed with 0.8 mmoles of TCMS in the glove box and injected in the desiccator maintained at relative humidity level of  $35\% \pm 1\%$ . Si wafers were used as a substrate and reaction was carried out for 4 hours. SEM was performed to analyze the surface of coated Si wafers. Figure 4a shows SEM image of as synthesized nanostructure, while Figure 4b shows its TEM image. The nanostructures have similar necklace structure when compared with AlNFs and are amorphous in nature as indicated by SAED (inset Figure 4b). To check the elemental composition of the synthesized nanostructures elemental mapping was performed at TEM. Figure 4c-d shows the TEM image and the corresponding elemental maps, while the overall EDX spectra is shown in Figure 4e. The maps shows presence of C, Al, O, Si and Cl. The carbon signal is supposed to be recorded from the presence of methyl groups of the TCMS precursor but it is hard to see the any contrast of carbon map<sup>[13][14]</sup>. The origin of Cl is probably due to the incomplete hydrolysis of the silane precursor or due to some adsorbed Cl. Chlorine was not detected when only TMA was used for the synthesis of AlNFs. The contamination of Al-SiFNs samples during TEM sample preparation is also not a possible reason because the same solvent (toluene) and procedure was applied for AlNFs and Al-SiFNs.

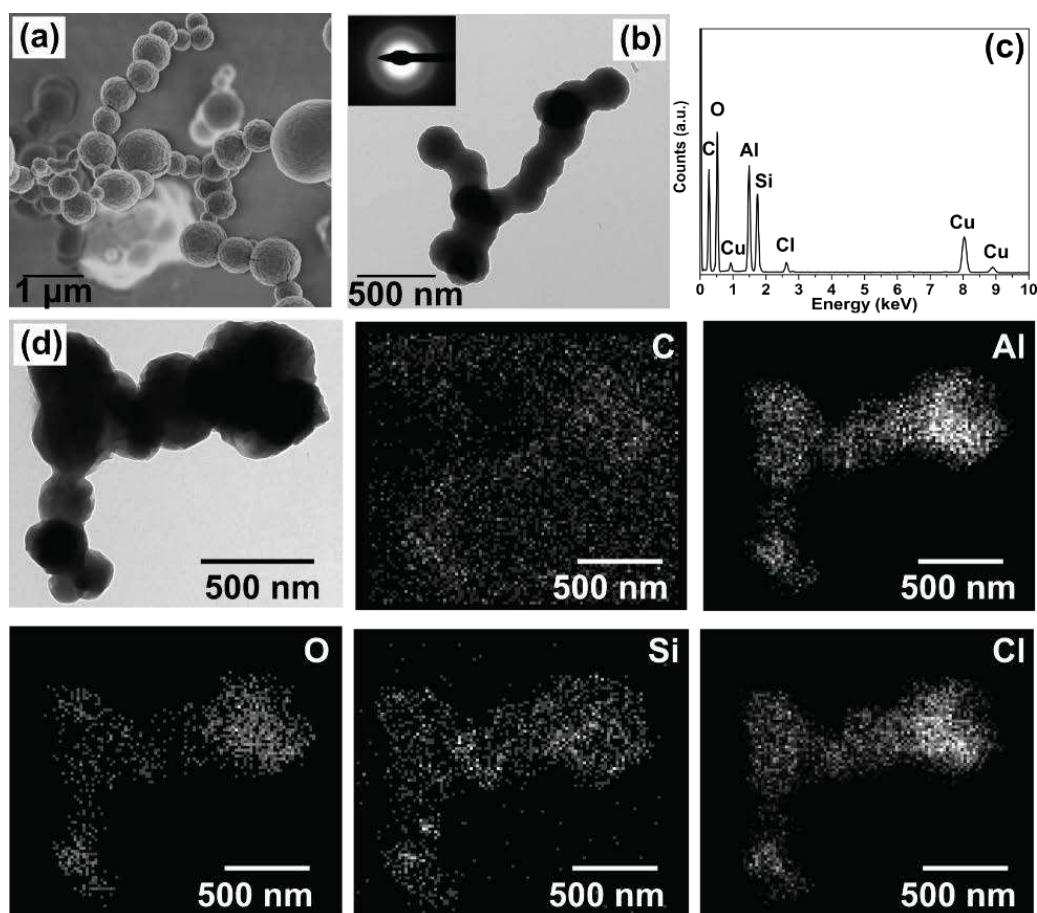


Figure 4: (a) SEM image of synthesized nanostructures by mixing TMA and TCMS, (b) TEM image (inset SAED), (c-d) TEM image, elemental mapping and the EDX spectra of nanostructures.

The source of Cl could be the grease which is used to seal the desiccator. For this purpose grease was pasted on aluminum stub and EDX analysis of grease was performed at EDAX system attached with SEM. EDX spectra revealed grease is composed of C, O and Si only (Figure 6 in supporting info). Even there was no presence of Cl when only TCMS was used for standard SNFs synthesis. TEM image, elemental mapping and EDX spectra of corresponding SNFs is shown in Figure 7 & 8 in supporting info. When only TCMS is used for DAGS, hydrolysis of silane results in formation of HCl gas. But in the presence of TMA presumably complete hydrolysis of TCMS does not occur which leads to presence of Cl in the synthesized nanostructures.

Relative humidity plays a vital role in DAGS chemistry. To check the influence of relative humidity on synthesis of Al-SiNFs synthesis at different relative humidity levels was carried

out. At humidity level of 2% no structures were obtained while at 17% necklace type structures were observed. The increase of humidity has the same influence on the synthesis of AlNFs as in the case of SNFs. At humidity levels of 50% and 70% particulate structures were obtained (Figure 9 supporting info). The deformed particulate type structures are obtained when silane reacts at high humidity levels leading to small particles with indefinite shapes. Figure 5 shows the TEM imaging and elemental mapping of Al-SiNFs synthesized at different humidity levels. The same observation can be made in SEM and TEM micrographs showing presence of irregular shaped particles at high humidity levels. Elemental mapping also shows inhomogeneous distribution of elements inside the nanostructures due uncontrolled reaction of TMA and TCMS at high humidity levels.

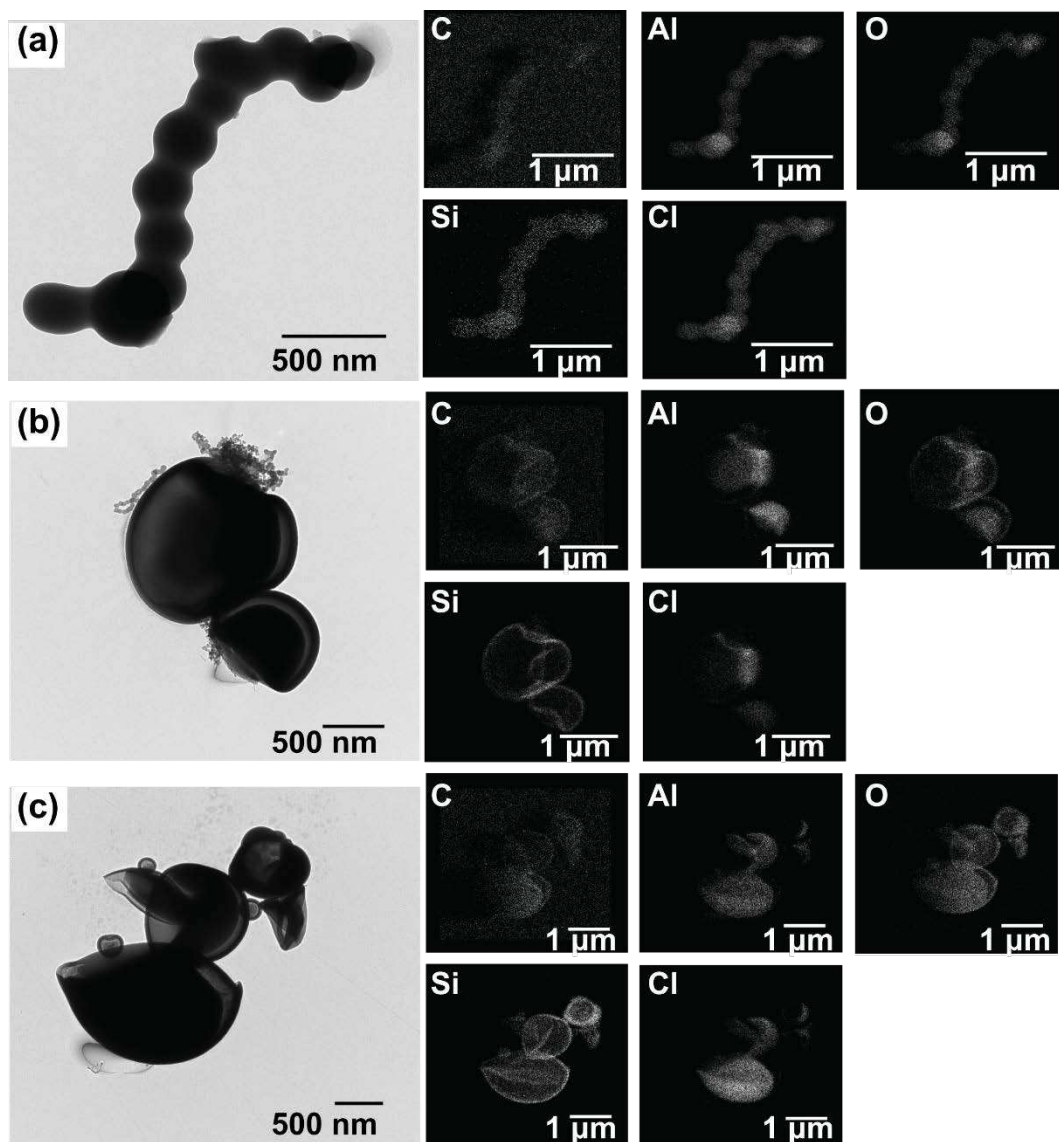


Figure 5: TEM and elemental mapping of Al-SiNFs synthesized at humidity levels of (a) 17%, (b) 50% and (c) 70%.

The growth behavior of Al-SiNFs was studied by stopping the reaction after 15 and 30 minutes of precursor injection. After 15 minutes of reaction time small particulate structures were formed with protrusions at the outer surface (Figure 6a & c).



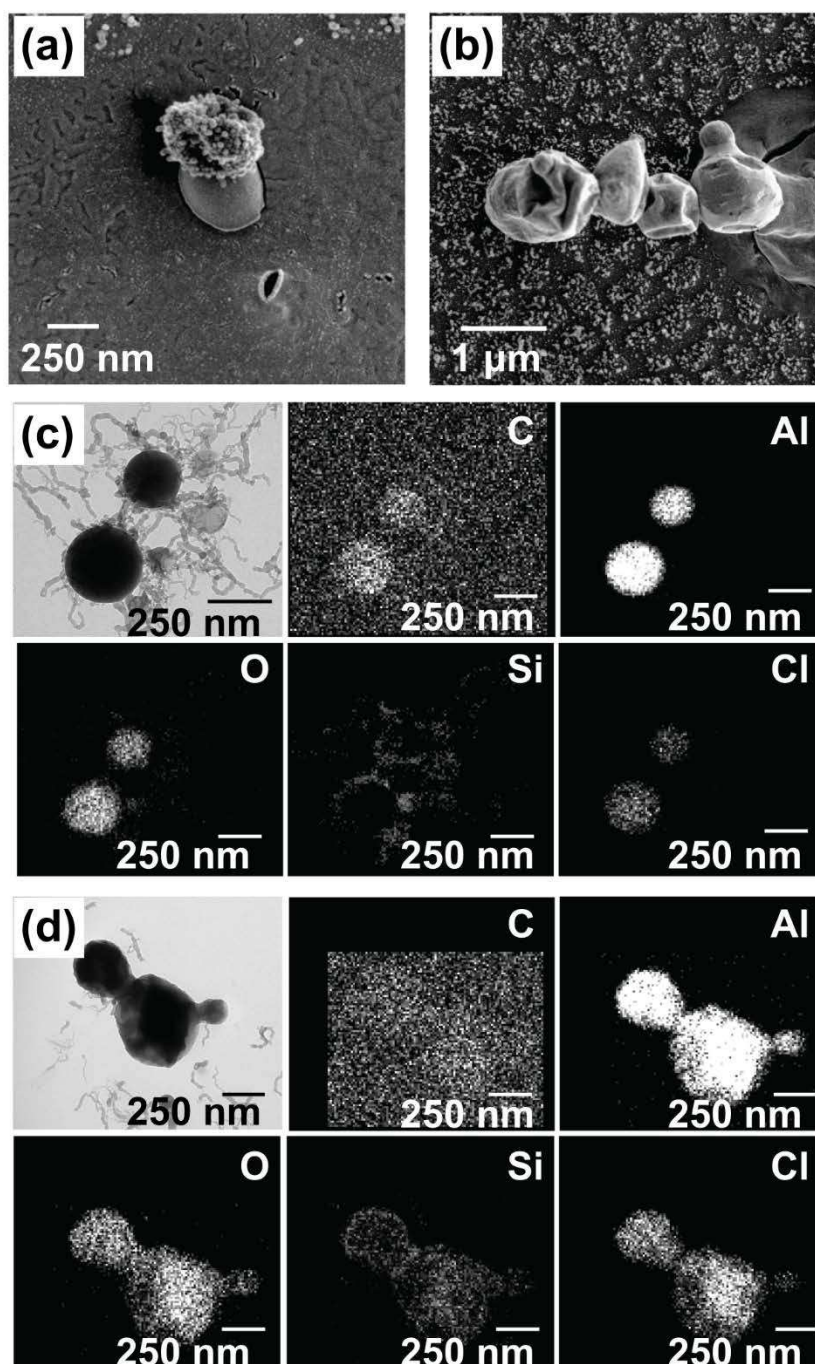


Figure 6: SEM image of Al-SiNFs synthesized after (a) 15 min, (b) 30 min, TEM image and elemental mapping after (c) 15 min, (d) 30 min of reaction time

After 30 minutes small particulate structures start to grow further making necklace type structures. TEM of the synthesized nanostructures also shows presence of protrusions at the surface of particles after 15 minutes of reaction. The elemental mapping done reveals the protrusions are composed of Si however the particles are made of Al. Due to the high reactivity of TMA, aluminum based particles are formed in the beginning and the silane molecules react

with these particles (as observed in the form of protrusions). With the passage of time precursors react further leading to formation of necklace/bead type structure. This also explains why Al-SiNFs & AlNFs have similar structure. The growth behavior of Al-SiNFs was also studied after 1 or 2 hours of reaction time but no significant difference in the structures was observed when compared with structures synthesized after 4 hours of reaction time.

### **FTIR and NMR measurements**

For FTIR analysis Ge wafers were used for the synthesis instead of Si to eliminate the possibility of Si-O-Si signal from the substrate. Figure 7 shows FTIR spectra of AlNFs, Al-SiNFs and SNFs. The signal from the substrate around  $840\text{ cm}^{-1}$  can be observed in both spectra indicating Ge-O-Ge bond stretching<sup>[31]</sup>. In AlNFs peaks at  $600\text{ cm}^{-1}$  and  $965\text{ cm}^{-1}$  are detected which show the bond stretching of Al-O-Al<sup>[32]</sup>. The peaks originating from hydroxyl groups (-OH) can also be seen in AlNFs around  $1600\text{ cm}^{-1}$  and  $3300\text{ cm}^{-1}$ . In Al-SiNFs some new peaks are observed in addition to the Al-O-Al, Ge-O-Ge and -OH bond vibrations. By comparing the FTIR spectra of Al-SiNFs with SNFs we observe the presence of Si-O-Si stretching in both material systems. Si-O-Si bond vibrations and stretching are observed at  $787\text{ cm}^{-1}$  and  $904\text{ cm}^{-1}$  respectively<sup>[33]</sup>. However the Si-O-Si stretching at  $1020\text{ cm}^{-1}$  and  $1125\text{ cm}^{-1}$  which are observed in SNFs are slightly shifted in Al-SiNFs. In Al-SiNFs the peaks are shifted to  $1036\text{ cm}^{-1}$  and  $1132\text{ cm}^{-1}$ . The shift in Si-O-Si peaks indicates presence of Al in the network of Si-O-Si in Al-SiNFs. The Si-O-Si shift is reported in literature for aluminosilicate structures, but these shifts do not provide a concrete evidence of the presence of Al-O-Si bonding<sup>[34][35]</sup>. In addition, peaks at  $1270\text{ cm}^{-1}$  and  $3000\text{ cm}^{-1}$  are also observed in Al-SiNFs and SNFs which indicate the Si-CH<sub>3</sub> and -CH<sub>3</sub> stretching respectively<sup>[36][37]</sup>. These peaks are originated because of methyl groups of silane.



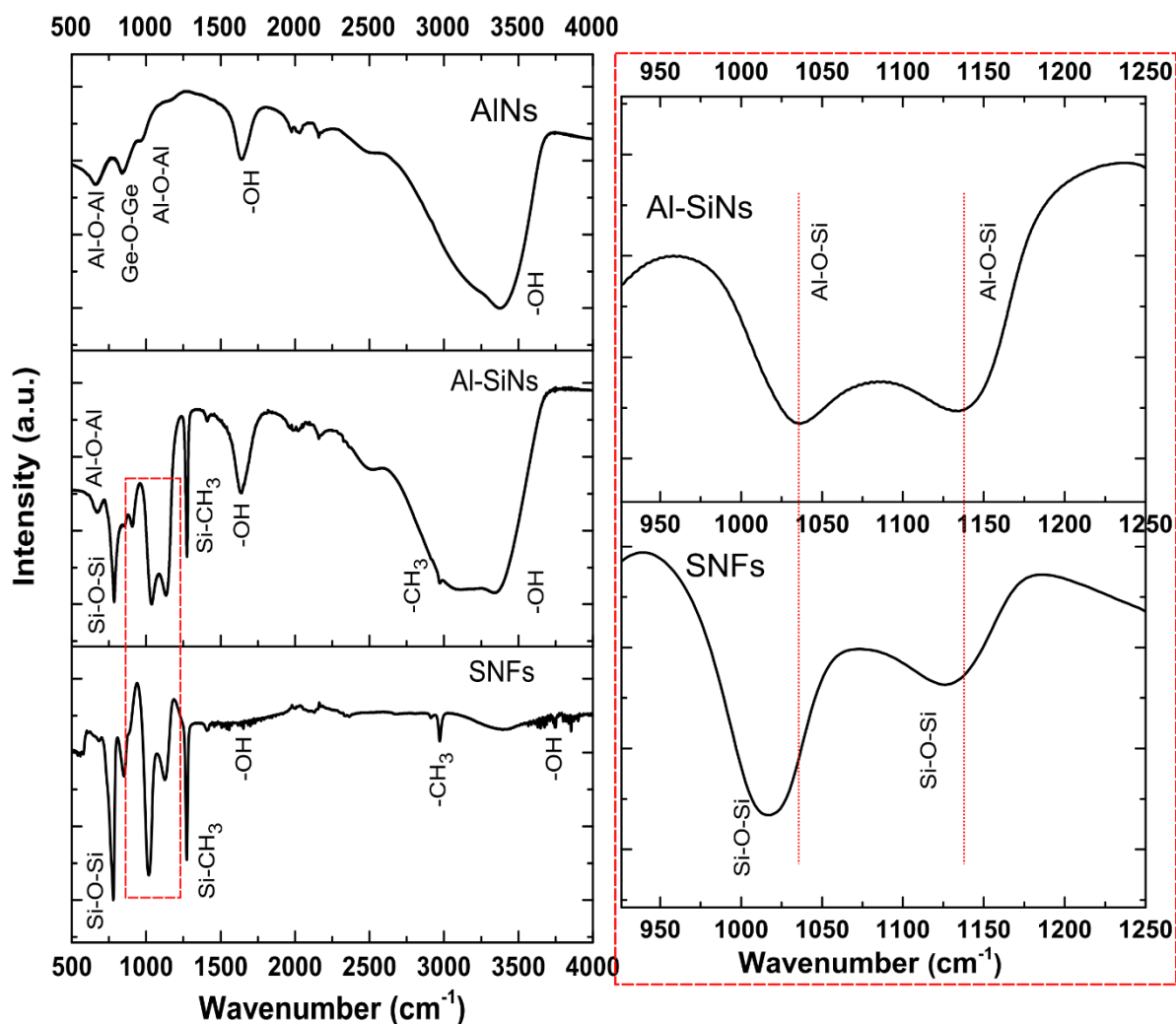


Figure 7: FTIR spectra of AlNFs, Al-SiNFs and SNFs and magnified spectra of highlighted region

For the precise information about the presence of bonding between atoms of synthesized nanostructures, solid state NMR measurements were performed.  $^{29}\text{Si}$  NMR is a very useful technique to accurately determine the bonding of Si with other atoms.  $^{29}\text{Si}$  NMR spectra of SNFs and Al-SiNFs is shown in Figure 8. Three peaks were observed for both SNFs and Al-SiNFs. The peaks located at -48.28, -59.0 and -68.68 ppm were observed for SNFs while for Al-SiNFs peaks at -48.95, -59.0 and -68.93 ppm were observed. These peaks indicate the typical silicone peaks in silanes also known as T region<sup>[38]</sup>. The peaks around -48 ppm indicate one fold Si-O linkage in silicone, while peaks at -59 ppm show two fold Si-O linkage in silicone<sup>[38][39][40][41]</sup>. The peaks at 68 ppm indicate three fold Si-O linkage showing condensation

of hydroxyl group of silanes<sup>[38][39][40][41]</sup>. As observed in the given  $^{29}\text{Si}$  NMR spectra, the T peaks were observed for both SNFs and Al-SiNFs with minor shifts which indicate the chemical surrounding of Si in both nanostructures is similar. Usually, the addition of Al into the network of silicates leads to a chemical shift as observed by Lippmaa et al<sup>[42]</sup>. Lippmaa et al reported that addition of one Al atom into the network of silicate leads to a chemical down shift of 5-6 ppm which adds up by the addition of every Al atom<sup>[42][43]</sup>. However, the as synthesized SNFs and Al-SiNFs do not show an appreciable chemical shift which provides a strong evidence of the existence of mixed structure instead of Al-O-Si bonding.

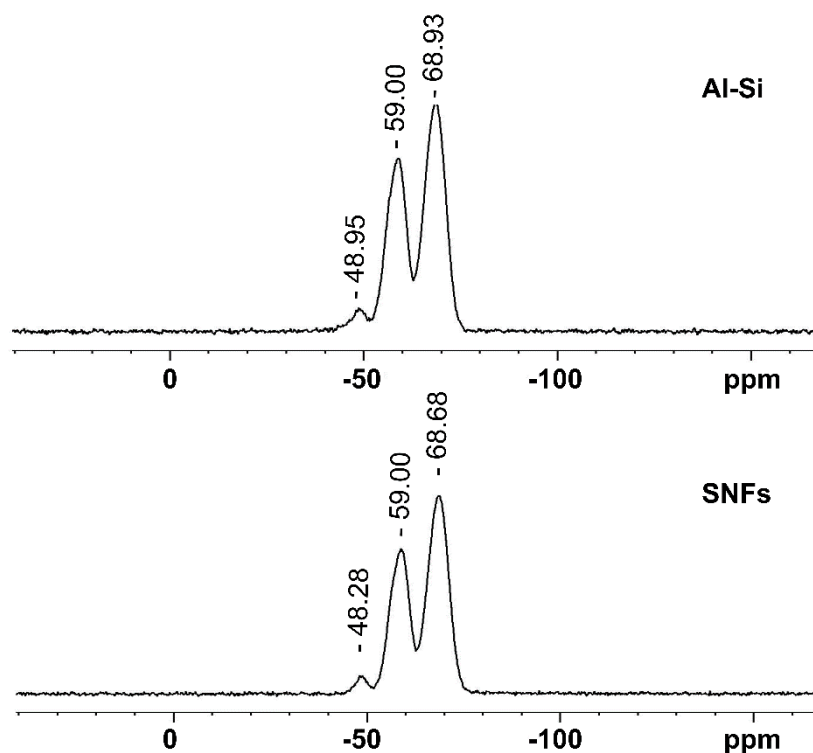


Figure 8:  $^{29}\text{Si}$  NMR spectra of SNFs and Al-SiNFs

Annealing of Al-SiNFs was performed in air to check their thermal stability. The coated wafers were heated at 300°C, 400°C, 500°C and 600°C at the heating rate of 10°C/min. All samples were annealed for 4 hours followed by cooling in the furnace. It was observed with the increase of annealing temperature aggregation and degradation of nano-necklaces was observed. **Figure 10 in supporting info** shows with the increase of annealing temperature aggregation occurred.

TEM shows with the increase of annealing temperature nanostructures degrade ([supporting info Figure 11 & Figure 12](#)). Structural changes occur after annealing which lead to inhomogeneous distribution of Al and Cl in the nanostructures. It is presumably due to the hydrolysis and condensation of hydroxyl groups. However, this requires further investigation to understand the mechanisms behind thermal degradation.

## Conclusions

We have shown for the first time the synthesis of a new category of 1D nanomaterials using Droplet Assisted Growth and Shaping mechanism. Al and mixed Al-Si bead type nanostructures have been synthesized in a custom build chamber. The humidity inside the chamber played an important role for the synthesis of nanostructures. EDX analysis has revealed homogenous composition of elements inside the nanostructures. These results are well supported by observations made by NMR and FTIR spectroscopy. The analytical data show that the mixed nanostructures consist mainly of separated Si- and Al-containing macromolecules; the existence of Al-O-Si-groups could not clearly demonstrated. The synthesized nanostructures are not thermally stable when heated in air and degrade with increase of annealing temperature. This work does not only show the synthesis of Al-containing nanostructures obtained by a convenient and straightforward process. Beyond this, it is a clear demonstration that the DAGS synthesis mechanism is not restricted to a single class of chemical substances but rather a promising pathway covering a broad range of chemical elements. Subsequently to the demonstration of the synthesis of Si-, Ge-, Al- and Al-Si containing nanostructures, further work is underway to extend the DAGS synthesis mechanism to other components.

## References

- [1] R. E. Morris, P. S. Wheatley, *Angew. Chemie Int. Ed.* **2008**, 47, 4966.
- [2] J. Luryi, S; Xu, *Future Trends in Microelectronics*, WILEY-VCH Verlag, New York, **2002**.
- [3] X. Lu, C. Wang, Y. Wei, *Small* **2009**, 5, 2349.
- [4] L. R. Zhao, C. Li, J. Xu, W. G. Wu, in *2013 13th IEEE Int. Conf. Nanotechnol. (IEEE-NANO 2013)*, **2013**, pp. 582–585.
- [5] R. D. Piner, J. Zhu, F. Xu, S. Hong, C. A. Mirkin, *Science* (80-. ). **1999**, 283, 661 LP.
- [6] J.-F. Liu, X.-L. Li, Y.-D. Li, *J. Cryst. Growth* **2003**, 247, 419.
- [7] J. Kim, S. A. Yang, Y. C. Choi, J. K. Han, K. O. Jeong, Y. J. Yun, D. J. Kim, S. M. Yang, D. Yoon, H. Cheong, K.-S. Chang, T. W. Noh, S. D. Bu, *Nano Lett.* **2008**, 8, 1813.
- [8] A. Baji, Y.-W. Mai, Q. Li, Y. Liu, *Nanoscale* **2011**, 3, 3068.
- [9] R. Brukh, S. Mitra, *Chem. Phys. Lett.* **2006**, 424, 126.
- [10] S. Christiansen, R. Schneider, R. Scholz, U. Gösele, T. Stelzner, G. Andrä, E. Wendler, W. Wesch, *J. Appl. Phys.* **2006**, 100, DOI 10.1063/1.2357342.
- [11] C.-J. Kim, K. Kang, Y. S. Woo, K.-G. Ryu, H. Moon, J.-M. Kim, D.-S. Zang, M.-H. Jo, *Adv. Mater.* **2007**, 19, 3637.
- [12] S. Y. Bae, H. W. Seo, J. Park, *J. Phys. Chem. B* **2004**, 108, 5206.
- [13] G. R. J. Artus, S. Jung, J. Zimmermann, H.-P. Gautschi, K. Marquardt, S. Seeger, *Adv. Mater.* **2006**, 18, 2758.
- [14] G. R. J. Artus, S. Seeger, *Adv. Colloid Interface Sci.* **2014**, 209, 144.
- [15] S. Oliveira, A. Stojanovic, *J. Nanoparticle Res.* **2018**, 20: 307.
- [16] G. R. J. Artus, S. Seeger, *Ind. Eng. Chem. Res.* **2012**, 51, 2631.
- [17] J. Zimmermann, F. A. Reifler, G. Fortunato, L.-C. Gerhardt, S. Seeger, *Adv. Funct. Mater.* **2008**, 18, 3662.
- [18] D. E. Rollings, J. G. C. Veinot, *Langmuir* **2008**, 24, 13653.
- [19] J. Zhang, S. Seeger, *Angew. Chemie Int. Ed.* **2011**, 50, 6652.
- [20] Z. Chu, Y. Feng, S. Seeger, *Angew. Chemie Int. Ed.* **2015**, 54, 2328.
- [21] G. R. Meseck, R. Kontic, G. R. Patzke, S. Seeger, *Adv. Funct. Mater.* **2012**, 22, 4433.
- [22] N.-H. Saddiqi, D. Patra, S. Seeger, *Colloid Interface Sci. Commun.* **2017**, 16, 1.
- [23] A. S. M. Meier, S. Seeger, *Small* **2017**, 13, 1601072.
- [24] J. Zimmermann, M. Rabe, D. Verdes, S. Seeger, *Langmuir* **2008**, 24, 1053.
- [25] G. R. J. Artus, S. Oliveira, D. Patra, S. Seeger, *Macromol. Rapid Commun.* **2017**, 38,

1600558.

- [26] N.-H. Saddiqi, D. Patra, S. Seeger, *ChemPhysChem* **2019**, *20*, 538.
- [27] D.-Y. Kang, N. A. Brunelli, G. I. Yucelen, A. Venkatasubramanian, J. Zang, J. Leisen, P. J. Hesketh, C. W. Jones, S. Nair, *Nat. Commun.* **2014**, *5*, 3342.
- [28] Q. Qin, T. Kim, X. Duan, J. Lian, W. Zheng, *Cryst. Growth Des.* **2016**, *16*, 6139.
- [29] N. Jeong, S. Hong, C. Kim, K. Kim, *J. Am. Ceram. Soc.* **2015**, *98*, 4036.
- [30] M. James, T. A. Darwish, S. Ciampi, S. O. Sylvester, Z. Zhang, A. Ng, J. J. Gooding, T. L. Hanley, *Soft Matter* **2011**, *7*, 5309.
- [31] S. J. L. R. Denise T. B. De Salvi, Aldo E. Job, *J. Brazilian Chem. Soc.* **2015**, *26*, 992.
- [32] O. M. C. Reyes, Carlos Alberto Ríos, Williams, Craig, & Alarcón, *Mater. Res.* **2013**, *16*(2), 424.
- [33] A. ADAMCZYK, *Mater. Sci.* **2015**, *33*, 732.
- [34] P. Padmaja, G. M. Anilkumar, P. Mukundan, G. Aruldas, K. G. K. Warriar, *Int. J. Inorg. Mater.* **2001**, *3*, 693.
- [35] P. P. Nampi, P. Moothetty, F. J. Berry, M. Mortimer, K. G. Warriar, *Dalt. Trans.* **2010**, *39*, 5101.
- [36] R. Chen, X. Zhang, Z. Su, R. Gong, X. Ge, H. Zhang, C. Wang, *J. Phys. Chem. C* **2009**, *113*, 8350.
- [37] G. P. Bhaskar J. Saikia, *J. Mod. Phys.* **2010**, *1*, 206.
- [38] F. Bauer, H.-J. Gläsel, U. Decker, H. Ernst, A. Freyer, E. Hartmann, V. Sauerland, R. Mehnert, *Prog. Org. Coatings* **2003**, *47*, 147.
- [39] I. Mora-Barrantes, J. L. Valentín, A. Rodríguez, I. Quijada-Garrido, R. Paris, *J. Mater. Chem.* **2012**, *22*, 1403.
- [40] T. M. Arantes, A. H. Pinto, E. R. Leite, E. Longo, E. R. Camargo, *Colloids Surfaces A Physicochem. Eng. Asp.* **2012**, *415*, 209.
- [41] C.-Y. C. Hsing-I Hsiang, *J. Am. Ceram. Soc.* **2008**, *91*, 387.
- [42] E. Lippmaa, M. Maegi, A. Samoson, G. Engelhardt, A. R. Grimmer, *J. Am. Chem. Soc.* **1980**, *102*, 4889.
- [43] W. W.-L. Shao, NMR Studies of Amorphous Silicon and Aluminosilicate Glass, Iowa State University, **1989**.